A Novel In-Service Surveillance Scheme for Optically Amplified Transmission Systems

Chun-Kit Chan, *Student Member, IEEE*, Lian-Kuan Chen, *Member, IEEE*, Frank Tong, *Senior Member, IEEE*, and Dennis Lam

Abstract—**We propose here a novel surveillance scheme for an optically amplified transmission system which allows simultaneous in-service fault identification for fiber and optical amplifiers. While requiring additional fiber Bragg gratings of designated wavelengths to be integrated with optical amplifiers, the monitoring light source is derived from the unused spectra of ASE and no dedicated light source is needed as in conventional OTDR technique. We have further demonstrated the scheme's feasibility with a 100-km, three-EDFA optical transmission system.**

Index Terms—**Fault diagnosis, optical fiber testing.**

I. Introduction

IN LONG-DISTANCE optical transmission systems operating at 1.55 μm, erbium-doped fiber amplifiers (EDFA's) are usually used to compensate the fiber loss and extend the transmission distance. It is thus desirable to implement a practical surveillance scheme to provide in-service monitoring of each amplifier's status and identify any fiber breaks in the transmission system.

Several approaches in EDFA status-monitoring and fiber fault identification were proposed previously [1], [2]; but these schemes require an extra light source dedicated for the monitoring function. Besides, multiple nonstandard bidirectional optical amplifiers are needed for the reflected monitoring signals [1], since the standard EDFA is equipped with an optical isolator which suppresses the reflected monitoring signals from reaching the sensor. Another approach [3] applies direct modulation on the pump laser, but this method can only monitor the pump condition and fails to identify any fiber cut. Recently, we have proposed an in-service surveillance scheme [4] for optically-amplified branched networks using fiber Bragg gratings (FBG) as the segment/amplifier identifiers and the amplified spontaneous emission (ASE) from the off-signal-transmission-band of the EDFA as the light source. Based on similar architecture but with very different operation principle, we propose and demonstrate here a novel in-service surveillance scheme which provides both EDFA status monitoring and fiber fault identification in optical transmission systems. The complete surveillance scheme is passive and can be carried out simultaneously without suspending the in-service data channels.

Manuscript received March 11, 1997; revised July 10, 1997.

C.-K. Chan was with the Department of Information Engineering, The Chinese University of Hong Kong, Shatin, N.T., Hong Kong. He is now with the Department of Electronic Engineering, City University of Hong Kong, Kowloon, Hong Kong.

L.-K. Chen and F. Tong are with the Lightwave Communications Laboratory, Department of Information Engineering, The Chinese University of Hong Kong, Shatin, N.T., Hong Kong.

D. Lam is with JDS FITEL Inc., Nepean, ON, K2G 5W8 Canada.

Publisher Item Identifier S 1041-1135(97)07926-3.

II. Surveillance Scheme

Fig. 1(a) shows a typical optical transmission system with $N+1$ EDFA's (EDFA_0, $\text{EDFA}_1, \cdots$, EDFA_N) and N segments of fibers. Each EDFA consists of an erbium-doped fiber with a pump diode laser and an optical isolator placed at the output so as to minimize the gain perturbation caused by any ASE from downstream EDFA's. Usually the data traffic is transmitted within the flat-gain region (1540–1556 nm) of the EDFA. In standard EDFA, the gain spectra (1525–1540 nm, 1556–1566 nm) are not usually used since the gain profiles are not flat. Transmitting data in nonflat gain region creates the problem of gain variation among the channels. Therefore, we utilize the unused nonflat ASE spectra (about 25 nm) as the light source of our monitoring wavelengths in our proposed surveillance scheme. Our scheme requires an additional FBG to be positioned close to the input end of each EDFA except EDFA_0 which serves as the power amplifier [see Fig. 1(b)]. At each EDFA, if an input optical isolator is required, it should be placed in front of the FBG. The distinct FBG center wavelengths, $\lambda_1, \lambda_2, \cdots, \lambda_N$, assigned, respectively, to $\text{EDFA}_1, \text{EDFA}_2, \cdots, \text{EDFA}_N$, are chosen from EDFA's unused ASE spectra. These FBG wavelengths serve as the monitoring wavelengths. Since the nonflat gain regions we considered are still within the 3-dB bandwidth of EDFA, so the monitoring wavelength will not be severely attenuated.

To understand the operation principle, first we consider different ASE components at the ith EDFA. The forward ASE from the EDFA_{i-1} is filtered out by the FBG_i, resulting in a notch at λ_i in the input ASE spectrum to EDFA_i [Fig. 2(a), inset (i)]. Under normal operation, this notched input ASE spectrum induces a similar spectrum from EDFA_i emitting in both forward and backward directions. The backward ASE from EDFA_i is then reflected at λ_i by the FBG_i [Fig. 2(a), inset (ii)]. This reflection may compensate the reduced ASE spectrum at λ_i, and level off the distinct notch at λ_i in the overall output ASE spectrum of EDFA_i [Fig. 2(a), inset (iii)]. The details of the output spectra depend on various system parameters such as link distance, amplifier gain, etc. Without influence by the forward ASE from EDFA_{i-1} due to pump-laser degradation or a fiber break in segment L_i, the EDFA_i will emit its ASE normally without a deep notch at λ_i. Together with the reflection at λ_i, the resultant spectrum from EDFA_i has a strong enhanced emission at λ_i. The output spectra at the receiver end will thus be different from that of a

1041–1135/97$10.00 © 1997 IEEE

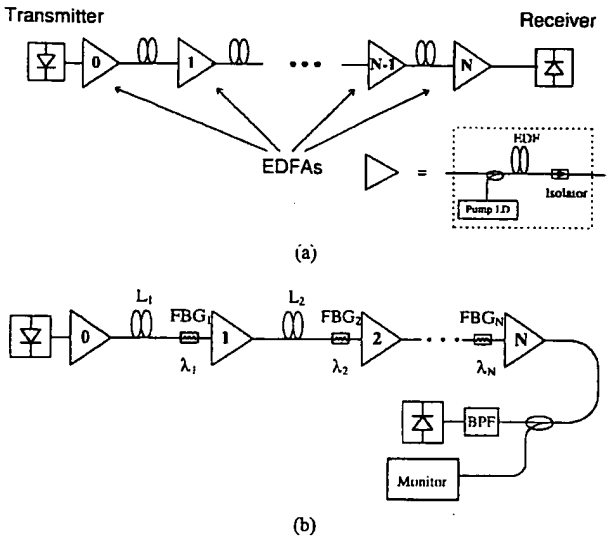

Fig. 1. (a) A typical optically amplified transmission system with $(N+1)$ EDFA's. (b) Our proposed surveillance system for optically amplified transmission system.

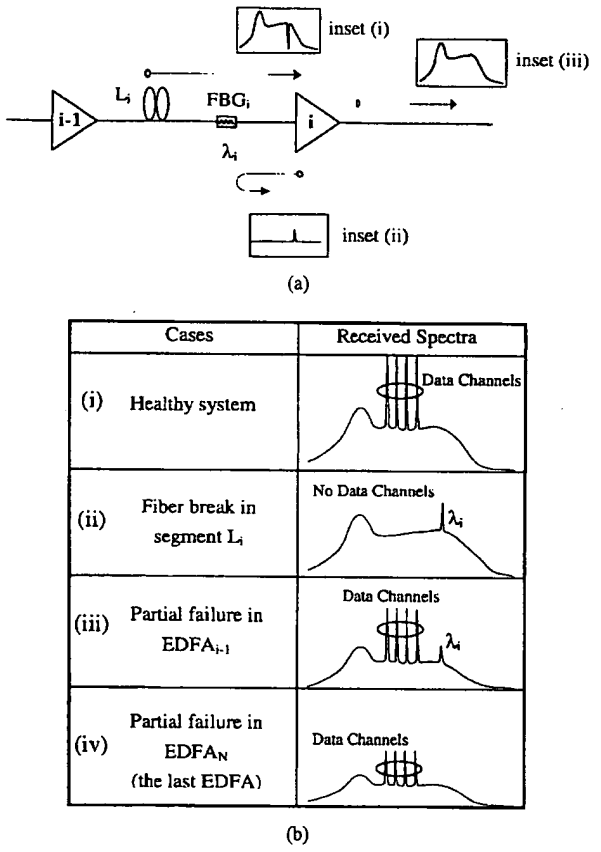

Fig. 2. (a) Operation principle of the proposed surveillance scheme. (b) Output spectra: (i) healthy system; (ii) fiber break in segment L_i; (iii) partial failure in EDFA$_i$; (iv) partial failure in EDFA$_N$.

healthy system, and these can be used for fault identification and EDFA status monitoring functions.

The output spectra at the receiver end under different system status are summarized and illustrated in Fig. 2(b). Consider a

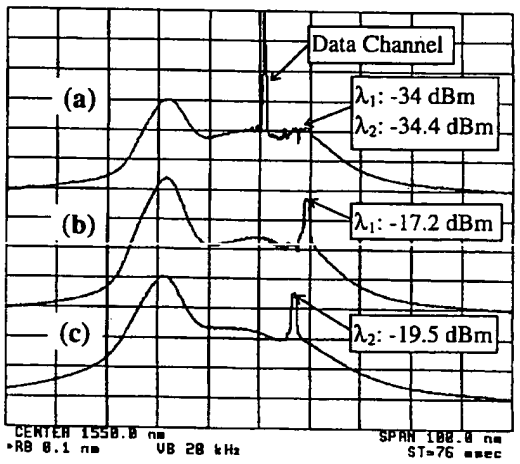

Fig. 3. Output spectra: (a) a healthy system, (b) fiber break in segment L_1 (power change at $\lambda_1 = +16.8$ dB), (c) fiber break in segment L_2 (power change at $\lambda_2 = +14.9$ dB). The data are taken at the receiver end. Note that the data channel is absent in (b) and (c).

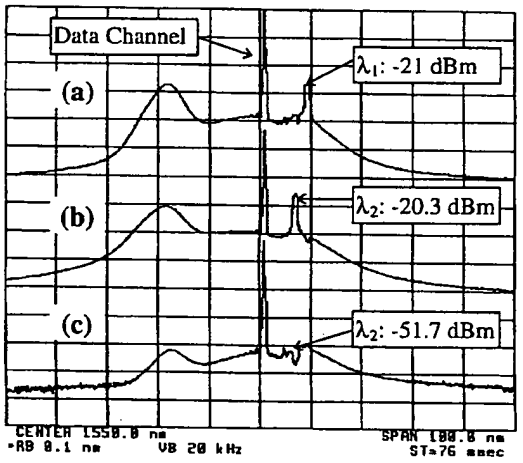

Fig. 4. Output spectra: (a) partial failure in EDFA$_0$ (power change at $\lambda_1 = +13$ dB), (b) partial failure in EDFA$_1$ (power change at $\lambda_2 = +14.1$ dB), (c) partial failure in EDFA$_2$ (power change at $\lambda_2 = -17.3$ dB).The data are taken at the receiver end.

fiber break in segment L_i, the data channels are absent from the final output spectrum since there is no signal being fed into EDFA$_i$ [Fig. 2(b), case(ii)]. As there is no ASE influence from EDFA$_{i-1}$, which is notched at λ_i, the FBG$_i$ can reflect a stronger ASE at λ_i and thus the enhanced emission at λ_i will be pronounced. For the case of partial failure in EDFA$_{i-1}$, except EDFA$_N$ (the last EDFA), and assuming no fiber break, there will be a power reduction in the whole ASE spectrum as input to EDFA$_i$, generating a strong enhanced emission at λ_i at the output of EDFA$_i$. In contrast to the fiber break case, the data channels are present in the final output spectrum [Fig. 2(b), case(iii)]. For a partial failure in the EDFA$_N$, there will be a significant power reduction in both data channels and monitoring wavelengths [Fig. 2(b), case(iv)]. By examining all the monitoring wavelengths continuously at the receiver end, simultaneous fiber fault identification and EDFA status monitoring can thus be achieved.

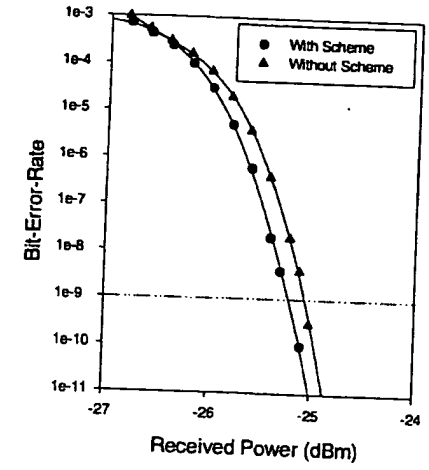

(a)

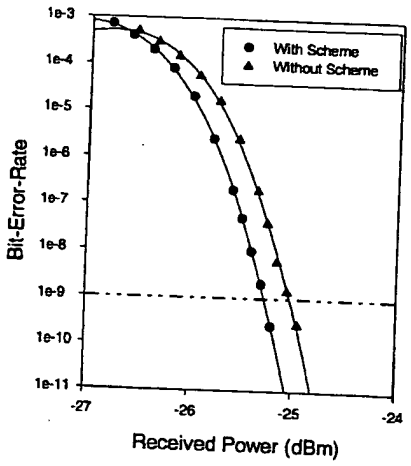

(b)

Fig. 5. BER performance of a 1-Gb/s ($2^{10}-1$ PRBS) NRZ data channel with (•) and without (▲) the surveillance scheme (a) under normal operation, (b) when $EDFA_1$ has a drop of 10 dB in gain due to pump laser degradation.

III. Experiments

The experimental setup is similar to that shown in Fig. 1(b) with altogether three EDFA's ($EDFA_0$, $EDFA_1$ and $EDFA_2$) and an EDFA spacing of 50 km, i.e., $L_1 = L_2 = 50$ km. The center wavelengths of FBG_1 and FBG_2 are $\lambda_1 = 1559.1$ nm and $\lambda_2 = 1556.8$ nm, respectively; and each FBG has a power reflectivity of 99.8% and a 3-dB full-width passband of 0.9 nm.

We use direct modulation on a DFB laser emitting at 1551 nm with a 1-Gb/s $2^{10}-1$ NRZ PRBS as the data channel. The average power of the data channel at the output of $EDFA_0$ is set at 4.95 dBm. The 50-km fiber separation yields about 10-dB loss which is compensated by the in-line EDFA, each operating with a net gain of about 10 dB. Trace (a) in Fig. 3 shows the output spectrum of a healthy system as observed at the monitor at the receiver end. The power levels of the monitoring wavelengths measured at λ_1 (−34 dBm) and λ_2 (−34.4 dBm) are recorded for reference. Traces (b) and (c) show the respective output spectra when L_1 and L_2 are intentionally disconnected to simulate a fiber break. The power levels at the monitoring wavelengths λ_1 and λ_2 are correspondingly raised by 16.8 dB to −17.2 dBm and by 14.9 dB to −19.5 dBm. Note that the data channel is absent in both spectra.

To demonstrate the EDFA status monitoring, the bias current of the pump laser of either $EDFA_0$ or $EDFA_1$ is reduced so as to produce a 10 dB drop in amplifier gain to simulate amplifier failure. After reducing the pump current in $EDFA_0$, the power level of the monitoring wavelength measured at λ_1 is raised by 13 dB to −21 dBm [see Fig. 4, trace (a)], indicating a partial failure of $EDFA_0$. In this case, the data channel is present. Similar result at λ_2 is obtained when pump current for $EDFA_1$ is reduced [Fig. 4, trace (b)]. When $EDFA_2$ (the last EDFA) is failed, the whole spectrum is reduced drastically [Fig. 4, trace (c)]. Bit error rate measurements are also performed for systems with and without the implementation of the surveillance scheme. An optical FP filter with a 3-dB bandwidth of 1 nm is placed before the photodiode to extract the data channel for BER measurement. No degradation in the data channel is observed under normal operation [Fig. 5(a)]. The apparent improvement of about 0.2 dB in BER performance is due to the reduction of ASE level by the in-line FBG's. In case of partial failure in an in-line EDFA, for instance, a 10-dB drop in gain at $EDFA_1$, the data channel is not degraded either [Fig. 5(b)].

IV. Summary

We have proposed and demonstrated a novel surveillance scheme for an optically amplified transmission system. The scheme is passive, nonintrusive, and allows simultaneous fault identification for fiber cut and failure of optical amplifiers. The proposed scheme is also practical and low cost since only additional FBG's are needed. The monitoring light source is derived from the unused spectra of ASE and no dedicated light source is needed as in conventional OTDR technique. The scheme is demonstrated successfully on a 100 km, three-EDFA optical transmission system. A high contrast of 13 dB in the monitoring signal power level is experimentally obtained between a healthy and a failed system. This greatly facilitates the detection process of the monitoring channels.

Acknowledgment

The authors would like to thank JDS-FITEL, Inc. for providing the fiber Bragg gratings.

References

[1] Y. W. Lai, Y. K. Chen, and W. I. Way, "Novel supervisory technique using wavelength-division-multiplexed OTDR in EDFA repeatered transmission systems," *IEEE Photon. Technol. Lett.*, vol. 6, pp. 446–449, Mar. 1994.

[2] Y. Sato and K. Aoyama, "Optical time domain reflectometry in optical transmission lines containing in-line Er-doped fiber amplifiers," *J. Lightwave Technol.*, vol. 10, pp. 78–83, Jan. 1992.

[3] S. Matsuoka, Y. Yamabayashi, and K. Aida, "Supervisory signal transmission methods for optical amplifier repeater systems," in *Proc. GLOBECOM'90*, 1990, paper 903.2.

[4] C. K. Chan, F. Tong, L. K. Chen, J. Song, and D. Lam, "A practical passive surveillance scheme for optically-amplified passive branched optical networks," *IEEE Photon. Technol. Lett.*, vol. 9, pp. 526–528, Apr. 1997.

A 1.6 μm Band OTDR Using a Synchronous Raman Fiber Amplifier

Toshiya Sato, Tsuneo Horiguchi, *Member, IEEE*, Yahei Koyamada, *Member, IEEE*, and Izumi Sankawa

Abstract—**A 1.6 μm band OTDR that is useful for optical transmission lines maintenance is reported. A synchronous Raman fiber amplifier (RFA) is employed to increase the dynamic range of the OTDR. Experimental results show that the dynamic range is extended to 25.7 dB with a spatial resolution of 100 m by using the RFA.**

I. Introduction

A 1.6 μm band OTDR offers good potential as test equipment for use in optical transmission system maintenance. This is because measurements at 1.6 μm are more sensitive to fiber macro- and micro-bending losses than those at 1.3/1.55 μm. This extra sensitivity allows anomalies to be detected in optical cables before they break down. By using test wavelengths that are different from communication wavelengths, it has become possible to test fibers, even in operating 1.3/1.55 μm WDM optical transmission systems [1]. However, the optical power of pulses from a conventional 1.6 μm laser diode (LD) is not very high and therefore no high dynamic range 1.6 μm OTDR has been developed. Recently, a synchronous Raman fiber amplifier (RFA) for 1.6 μm pulses has been reported [2]. A 1.55 μm pump pulse of more than 1 W is achieved with a synchronous RFA by using an erbium-doped fiber amplifier (EDFA), without the need to use a bulky high power laser such as a color center laser. Therefore, it is possible to incorporate the RFA in the OTDR for use in the field.

In this letter, we describe a 1.6 μm band OTDR which incorporates a synchronous RFA. The OTDR has a dynamic range of 25.7 dB which is achieved by using an RFA with a spatial resolution of 25.7 dB which is achieved by using an RFA with a spatial resolution of 100 m. This is 12.5 dB better than without the RFA.

II. Experiments

The RFA configuration is shown in Fig. 1. First, pump pulses are produced in the pump pulse generator by amplifying pulses from a 1.55 μm LD with an EDFA which is bidirectionally pumped at 1.48 μm. Then 1.66 μm LD pulses are input into the RFA and combined with the pump pulses with a WDM coupler. A timing controller is used to synchronize these combined pulses at the input to the Raman fiber. The Raman fiber was 14 km long with a mode field diameter (MFD) of 4.7 μm at 1.55 μm wavelength. The MFD is small compared with that of a normal dispersion shifted fiber. This is because the Raman effect is enhanced when a small MFD fiber is used. The dispersion of the Raman fiber at 1.6 μm was 56 ps/km/nm, resulting in a 100 ns difference between the transmission times of the 1.55 and 1.66 μm pulses through the Raman fiber. In order to avoid the decrease in gain due to the walkoff, the 1.55 μm pump pulse width was made 100 ns wider than the 1.66 μm signal pulse width. Finally, the transmitted pump pulse was filtered out using a long-wave-pass filter.

The configuration of a 1.6 μm band OTDR is shown in Fig. 2. The probe pulses from a 1.66 μm LD are amplified by the synchronous RFA and launched into a 20 km length of single mode test fiber through a directional coupler. The backscattered signals from the test fiber are received by an InGaAs avalanche-photodiode (APD) via the directional coupler, and converted to digital signals by an A/D converter. The digitized signals are averaged and displayed with a digital processing system.

III. Results and Discussion

First, the optical power of the 1.66 μm signal pulses, with and without the synchronous RFA, was measured with a calibrated photodiode and an oscilloscope. Fig. 3(a) and (b) show pulses with and without the RFA, respectively, for 1.6 μm band OTDR. It is seen in Fig. 3 that this RFA achieves an output optical peak power of 300 mW. However, the amplified pulse was deformed from a rectangular pulse to an exponentially decaying pulse. This is because the population inversion recovery of EDF is so late that the 1.55 μm pump pulse itself is exponentially decaying, and the gain of the RFA is in proportion to the pump power in decibels. The average optical power from the rising to the falling edge of the pulse is called effective power in this letter, because the OTDR signal power is in proportion to the average power. It is found from Fig. 3 that the effective power of the RFA output is 22.4 dBm and the effective RFA gain is +24.8 dB at a pulse width of 1.0 μs.

Second, the OTDR measurements were carried out at 1.66 μm with 2^{16} integrations, and with a pulse duration of 1.0 μs. Fig. 4 shows the backscattered signals for a 1.0 μs pulse duration both with and without the RFA. As can

Manuscript received April 8, 1992; revised May 11, 1992.
The authors are with NTT Telecommunications Field Systems R & D Center, Ibaraki-Ken 319-11, Japan.
IEEE Log Number 9201890.

1041-1135/92$03.00 © 1992 IEEE

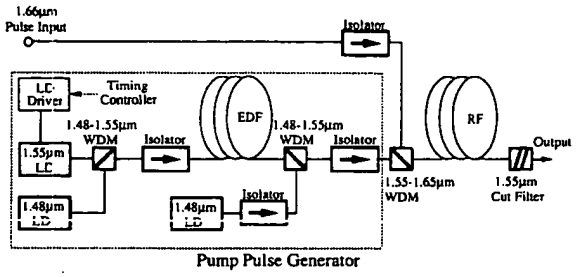

Fig. 1. Schematic configuration of the synchronous RFA.

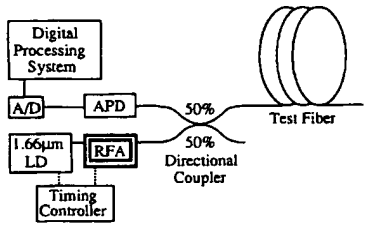

Fig. 2. Schematic configuration of a 1.6 μm band OTDR with synchronous RFA.

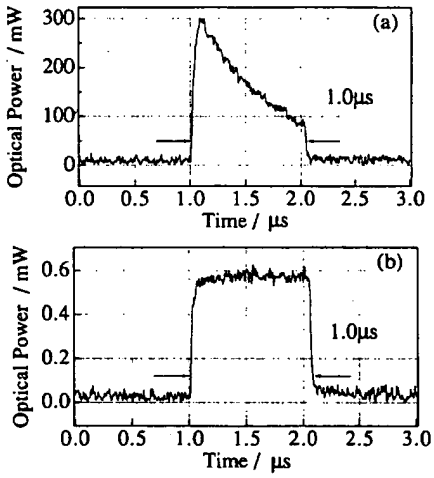

Fig. 3. Synchronous RFA amplification data. (a) With the RFA and (b) without the RFA.

be seen from Fig. 4, the OTDR dynamic range without the synchronous RFA was +13.2 dB. The range increased to +25.7 dB when the RFA was used, which is an improvement of +12.5 dB.

The OTDR dynamic range is calculated by using the following equation:

$$DR = \frac{P_{eff} - (R + C) - P_d + \frac{SNIR}{2}}{2} \quad [dB] \quad (1)$$

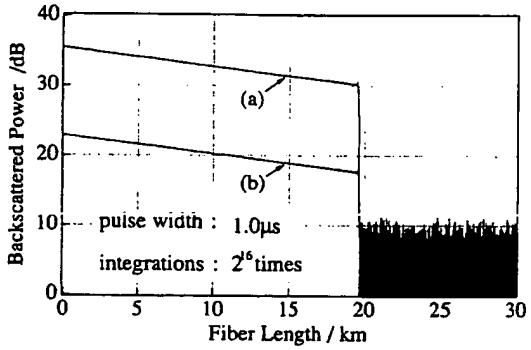

Fig. 4. Backscattered signals for a pulse duration of 1.0 μs. (a) With the RFA and (b) without the RFA.

where

P_{eff} : effective power of light source output (dBm)
P_d : minimum detectable optical power (~ -65.4 dBm for 1.0 μs)
R : Rayleigh scatter capture level ($\sim$ 54 dB for 1.0 μs)
C : roundtrip loss of directional coupler ($\sim$ 7.0 dB from experiments)
SNIR : postdetection S/N improvement (48 dB at 2^{16} integrations)

Then OTDR dynamic ranges with 2^{16} integrations are estimated by using (1). With and without the RFA the effective optical powers of the light source were -2.4 and 22.4 dBm, respectively. Therefore the OTDR dynamic ranges with and without the RFA were estimated as 13.0 and 25.4 dB, respectively. Fig. 4 shows that the OTDR dynamic ranges obtained experimentally agree with that predicted from the effective optical powers of the 1.66 μm signal pulses.

IV. Conclusion

A 1.6μm band OTDR incorporating a synchronous RFA which is key test equipment for optical transmission system maintenance has been demonstrated. By using a synchronous RFA an OTDR dynamic range of +25.7 dB was achieved in the 1.6 μm band with a pulse duration of 1.0 μs. The dynamic range of the OTDR with the RFA was +12.5 dB better than that without the RFA. This performance is approximately the same as that of commercially available 1.3/1.55 μm OTDR's.

Acknowledgment

The authors gratefully thank K. Ishihara for his encouragement during this work.

References

[1] Y. Koyamada, N. Ohta, and N. Tomita, "Basic concepts of fiber optic subscriber loop operation systems," in *Proc. Int. Conf. Commun.*, vol. 4, pp. 1540–1544, 1990.
[2] T. Horiguchi, T. Sato, and Y. Koyamada, "Stimulated Raman amplification of 1.6 μm band pulse light in optical fibers," *IEEE Photon. Technol. Lett.*, vol. 4, pp. 64–66, Jan. 1992.